charge-transfer band, not observed experimentally. Nevertheless the problem is further complicated in that the position of the a_{1g} (d_{z^2}) level depends critically upon whether the molecule is truly square planar with no near neighbors along the z axis or whether it is tetragonal with weak interactions along the z axis. Since the 1:2 nickel complex, according to X-ray data,[37,38] is N,N-coordinated forming five-membered rings, we could suggest a similar coordination for the ML species via the N atom of the amino group and the nitrogen atom of the deprotonated $-NHO^-$ group, as previously reported for nickel complexes of glycyl hydroxamic acid (aha)[15,39] and seryl hydroxamic acid (adhp).[30] The NiL_2 complex being square planar, the small difference in log K for NiL and NiL_2 species [$\Delta \log K$ (6.824 - 6.476) = 0.348] could be explained if we considered that it corresponds to an octahedral (NiL) to square-planar (NiL_2) transformation. In addition, the logarithm of the second stepwise formation constant (log K_2) for the Ni^{2+}-adhb system is appreciably greater than that of the first, log β_{101}. This is contrary to earlier findings[40-43] using a method of calculation based on the erroneous assumption that the formation of NiL is effectively complete before NiL_2 begins to be formed. The explanation of this behavior may lie in the ability of Ni^{2+} to form square-planar complexes; when a second ligand is bonding facially in a bidentate manner, the two five-membered chelate rings in the complex [NiL_2] are much more stable than one five-membered ring in the [NiL] species. In conclusion the X-ray crystal structures of two complexes of nickel(II)[37,38] and one of copper(II)[44] containing two glycyl hydroxamate anions (L^- = $H_2N-CH_2-CONHO^-$) provide evidence of coordination by the nitrogen amino and the nitrogen of the hydroxamate moiety for adhb and ahpp, respectively. Additional evidence for this type of coordination, which persists in solution, was given by potentiometric and spectrophotometric studies on nickel(II)[39,45] and copper(II).[31] We conclude therefore that M(II)adhb and M(II)-ahpp systems can probably satisfy different criteria for the biological activities and the analytical role proposed, giving a strong indication for the complexes investigated as being suitable sources of metal ions as trace elements that are essential in animal nutrition. Our results show clearly that, at physiological pH values, the assumption of an uncoordinated α-amino group in the M(II)-adhb and M(II)-ahpp systems is probably incorrect since the major species in this pH range is ML_2, which involves coordination of the α-amino group and hydroxamate $-NHO^-$ moiety.

Acknowledgment. Financial support in part by the Ministero della Pubblica Istruzione, Rome, and by the National Research Council of Italy (CNR) is gratefully acknowledged. I am greatly indebted to Professor P. Gans, Professor A. Vacca, and Professor A. Sabatini for their generous support of the program SUPERQUAD.

(40) Braibanti, A.; Dallavalle, F.; Leporati, E.; Mori, G. *J. Chem. Soc., Dalton Trans.* **1973**, 2539.
(41) Braibanti, A.; Dallavalle, F.; Leporati, E.; Mori, G. *J. Chem. Soc., Dalton Trans.* **1973**, 323.
(42) Braibanti, A.; Mori, G.; Dallavalle, F.; Leporati, E. *Inorg. Chim. Acta* **1972**, *6*, 106.
(43) Braibanti, A.; Dallavalle, F.; Leporati, E. *Inorg. Chim. Acta* **1969**, *3*, 459.
(44) De Miranda Pinto, C. O.; Paniago, E. B.; Tabak, M.; Carvalho, S.; Mascarenhas, Y. P. *Inorg. Chim. Acta* **1987**, *137*, 145.
(45) El-Ezaby, M. S.; Marafie, H. M.; Abud-Soud, H. M. *Polyhedron* **1986**, *5*, 973.
(46) *SAS User's Guide: Statistics*, Version 5; SAS Institute Inc.: Cary, NC, 1985; p 576.

Contribution from the Institute for Physical and Theoretical Chemistry, University of Frankfurt, Niederurseler Hang, 6000 Frankfurt/Main, FRG, Institute for Inorganic Chemistry, University of Witten/Herdecke, Stockumer Strasse 10, 5810 Witten, FRG, and Institut de Chimie Minérale et Analytique, Université de Lausanne, CH-1005 Lausanne, Switzerland

Kinetics and Mechanism of Solvent-Exchange and Anation Reactions of Sterically Hindered Diethylenetriamine Complexes of Palladium(II) in Aqueous Solution

J. Berger,[1a] M. Kotowski,[1a] R. van Eldik,*[1b] U. Frey,[1c] L. Helm,[1c] and A. E. Merbach*[1c]

Received February 16, 1989

The kinetics of water exchange on and anation reactions of $[Pd(R_5dien)H_2O]^{2+}$ (R_5dien = *N,N,N',N'',N''*-pentamethyl- and *N,N,N',N'',N''*-pentaethyldiethylenetriamine) by thiourea and methyl-substituted thiourea were studied as a function of temperature and pressure. The kinetic parameters (k, ΔH^*, ΔS^*, ΔV^*) for water exchange are as follows for R = Me and Et, respectively: 187 ± 27, 2.9 ± 0.1 s^{-1}; 62 ± 3, 63 ± 1 kJ mol^{-1}; +8 ± 7, −25 ± 2 J K^{-1} mol^{-1}; −7.2 ± 0.6, −7.7 ± 1.3 cm^3 mol^{-1}. The volumes of activation for the anation reactions of the pentamethyl and pentaethyl complexes are as follows (cm^3 mol^{-1}) for anation by thiourea, dimethylthiourea, and tetramethylthiourea, respectively: −9.3 ± 0.4, −8.3 ± 0.3; −9.1 ± 0.6, −10.2 ± 0.6; −13.4 ± 0.7, −12.7 ± 0.6. The negative volumes of activation are consistent with an associative mode of activation for both processes. Steric hindrance on either the dien ligand or the entering nucleophile does not affect the associative nature of the substitution process.

Introduction

Numerous studies from our laboratories and others have demonstrated the importance of including pressure as a kinetic parameter in the elucidation of inorganic reaction mechanisms.[2-4] These studies have especially led to a better understanding and a systematic classification of solvent-exchange and ligand-substitution reactions of octahedral complexes of transition-metal elements. It was for instance possible to reveal a mechanistic changeover for solvent-exchange and complex-formation reactions along the series of divalent first-row transition-metal complexes.[3] Furthermore, solvent-exchange reactions are of fundamental importance to ligand-substitution reactions that involve the replacement of a solvent molecule. They act as model systems for ligand-substitution reactions in which both the entering and leaving ligands are neutral molecules.

Some of us[1a,b] have a longstanding interest in the substitution behavior of sterically hindered diethylenetriamine complexes of palladium(II). Aspects that were investigated include spontaneous solvolysis reactions,[5,6] anation by anionic nucleophiles,[7] reactions

(1) (a) University of Frankfurt. (b) University of Witten/Herdecke. (c) Université de Lausanne.
(2) van Eldik, R., Ed. *Inorganic High Pressure Chemistry: Kinetics and Mechanisms*; Elsevier: Amsterdam, 1986; Chapters 2-4, and references cited therein.
(3) Merbach, A. E. *Pure Appl. Chem.* **1987**, *59*, 161.
(4) van Eldik, R.; Asano, T.; le Noble, W. J. *Chem. Rev.* **1989**, *89*, 549.

0020-1669/89/1328-3759$01.50/0

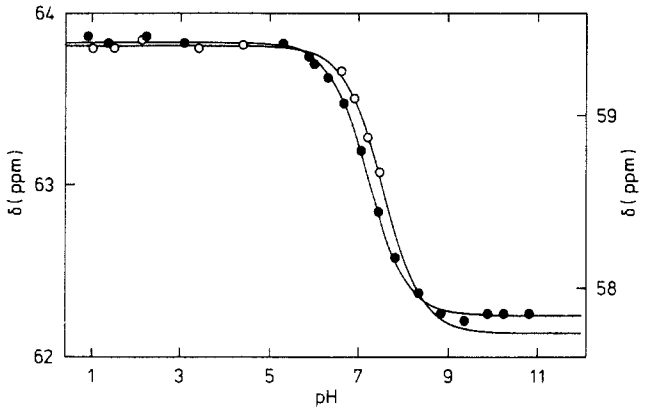

Figure 1. pH dependence of the chemical shift from the CH_2 (dien) ^{13}C NMR signals of $[Pd(Me_5dien)H_2O][ClO_4)_2$ (●; δ_{aquo} = 63.73 ± 0.01 ppm, $\delta_{hydroxo}$ = 62.14 ± 0.01 ppm) and $[Pd(Et_5dien)H_2O](ClO_4)_2$ (○; δ_{aquo} = 59.41 ± 0.01 ppm, $\delta_{hydroxo}$ = 57.73 ± 0.27 ppm).

with bicarbonate,[8] sulfite,[9] (tris(hydroxymethyl)amino)-methane,[10,11] and nucleic bases, nucleosides, and 5'-nucleotides,[12] substitution reactions at high pH,[13,14] construction of volume profiles for solvolysis reactions,[15] solvent dependence of solvolysis reactions,[16] and leaving-group effects on solvolysis reactions.[17] In contrast to octahedral systems, high-pressure data for solvent-exchange reactions on square-planar complexes are scarce.[2,18-21] A direct correlation between the kinetic parameters for solvent-exchange and anation reactions of sterically hindered palladium(II) complexes should significantly assist the interpretation of such data, especially in the case of the volume of activation for such processes. We have therefore studied the solvent-exchange and anation reactions of $[Pd(Me_5dien)H_2O]^{2+}$ and $[Pd(Et_5dien)H_2O]^{2+}$ (Me_5dien = *N,N,N',N'',N''*-pentamethyldiethylenetriamine; Et_5dien = *N,N,N',N'',N''*-pentaethyldiethylenetriamine), involving a series of neutral entering ligands, as a function of the usual kinetic variables, including pressure.

Experimental Section

Materials. The complexes $[Pd(Me_5dien)Cl]ClO_4$ and $[Pd(Et_5dien)Cl]ClO_4$ were prepared according to standard literature procedures.[22] They were subjected to chemical analyses[23] and the results were in excellent agreement with the theoretically expected values.[24] The chloro complexes were converted to the aqua analogues in solution by treating them with $AgClO_4$ according to the procedure described elsewhere.[8] Chemicals of analytical grade and doubly distilled water were used to prepare all solutions. $NaClO_4$ was used to adjust the ionic strength where indicated. ^{17}O-enriched water (Yeda) was used as received.

Measurements. UV–vis spectra were recorded on a Shimadzu UV 250 spectrophotometer. pH measurements were performed with a Metrohm E520 pH meter equipped with a glass electrode, the reference compartment of which was filled with 3 M NaCl (at the University of Frankfurt), and with a Metrohm E 603 pH meter equipped with a glass electrode and a calomel reference electrode using an agar-agar/$NaClO_4$ (1 M) gel electrolyte bridge (at the Université de Lausanne). The kinetics of the anation reactions were studied in the thermostated (±0.1 °C) cell compartment of the Shimadzu spectrophotometer or on a modified Aminco stopped-flow instrument at ambient pressure. A Zeiss DMR 10 spectrophotometer equipped with a thermostated (±0.1 °C) high-pressure cell[25] and a homemade high-pressure stopped-flow unit[26] were used to perform the kinetic measurements at elevated pressure (up to 150 MPa).

^{13}C NMR spectra were recorded by using a Bruker CXP-200 spectrometer with a 4.7-T wide-bore cryomagnet working at 50.3 MHz. ^{17}O NMR spectra were obtained on a Bruker AM-400 instrument that was equipped with a wide-bore cryomagnet (9.4 T) and was operated at 54.2 MHz. The ambient-pressure measurements were followed in commercial thermostated probe units, and the temperature was found constant within ±0.3 K as measured by a substitution technique.[27] Variable-pressure measurements were made up to 200 MPa by using a high-pressure probe.[28] The fast-injection measurements were made with use of the equipment described before.[29]

The $^{13}C\{^1H\}$ NMR spectra were obtained with use of pulse widths of 10 μs in the quadrature detection mode. We used 8K data points resulting from 100–500 scans accumulated over a total spectral width of 10 kHz. To improve the signal to noise ratio, we used an exponential filter (line broadening) of 4 Hz.

The variable-temperature (variable-pressure) ^{17}O NMR spectra were obtained with use of pulse widths of 14 μs (15 μs) in the quadrature detection mode. In both cases we used 2K data points resulting from the accumulation of 40 000–400 000 scans. The total spectral width was 83 kHz (50 kHz). A line broadening of 5–10% of the line width at half height, $\Delta\nu_{1/2}$, of the coordinated H_2O signal was applied. The NMR signal was fitted to a Lorentzian curve, and the transverse relaxation rate, $1/T_{2b}$, of the H_2O coordinated to Pd(II) was obtained from $\Delta\nu_{1/2}$, corrected for the line broadening (LB) by using the relation $1/T_{2b} = \pi(\Delta\nu_{1/2} - LB)$. The fast-injection spectra were obtained under the same conditions as for the variable-temperature measurements. However, only 500 scans with 0.125K data points were accumulated.

Results and Data Treatment

Water-Exchange Reactions. Variable pH. The acid dissociation constants K_a of $[Pd(Me_5dien)H_2O]^{2+}$ and $[Pd(Et_5dien)H_2O]^{2+}$ were obtained from the pH dependence of the $^{13}C\{^1H\}$ chemical shifts. The aqua and the hydroxo species are in fast exchange on the NMR time scale, due to a fast protonation/deprotonation process, and therefore only an average chemical shift δ can be measured. In both cases the dien CH_2 shift, which shows the largest chemical shift change during the titration, was selected. The shift variation is given by eq 1, where δ_{aqua} and $\delta_{hydroxo}$ are

$$pH = pK + \log\{(\delta - \delta_{hydroxo})/(\delta_{aqua} - \delta)\} \quad (1)$$

the unknown chemical shifts of the aqua and hydroxo species, respectively. This equation was least-squares fitted to the experimental data (supplementary material, Table SI) with pK_a, δ_{aqua}, and $\delta_{hydroxo}$ as adjustable parameters leading to pK_a values of 7.19 ± 0.03 for $[Pd(Me_5dien)H_2O]^{2+}$ and 7.53 ± 0.09 for the $[Pd(Et_5dien)H_2O]^{2+}$ complex. The larger error for the second case is due to the lack of data at higher pH caused by reversible precipitation for pH > pK_a. All experimental data and the calculated shifts are shown in Figure 1.

Variable Temperature. The ^{17}O NMR spectrum of a dilute aqueous solution of an aqua complex with slow water-exchange rate consists of two resonances: an intense peak due to the bulk water and a small broadened peak due to the coordinated water. This small peak is hard to detect and to line shape analyze, especially if the chemical shift difference is small. By addition of Mn^{2+}, a very efficient relaxation agent, the bulk water relaxes

(5) Breet, E. L. J.; van Eldik, R. *Inorg. Chem.* **1984**, *23*, 1865.
(6) Kotowski, M.; van Eldik, R. *Inorg. Chem.* **1984**, *23*, 3310.
(7) Breet, E. L. J.; van Eldik, R.; Kelm, H. *Polyhedron* **1983**, *2*, 1181.
(8) Mahal, G.; van Eldik, R. *Inorg. Chem.* **1985**, *24*, 4165.
(9) Mahal, G.; van Eldik, R. *Inorg. Chem.* **1987**, *26*, 1837, 2838.
(10) Breet, E. L. J.; van Eldik, R. *Inorg. Chem.* **1987**, *26*, 4264.
(11) Pienaar, J. J.; Breet, E. L. J.; van Eldik, R. *S. Afr. J. Sci.* **1988**, *84*, 389.
(12) Breet, E. L. J.; van Eldik, R. *Inorg. Chem.* **1987**, *26*, 2517.
(13) Breet, E. L. J.; van Eldik, R.; Kelm, H. *Inorg. Chim. Acta* **1984**, *85*, 151.
(14) Pienaar, J. J.; Breet, E. L. J.; van Eldik, R. *Inorg. Chim. Acta* **1989**, *155*, 249.
(15) Pienaar, J. J.; Kotowski, M.; van Eldik, R. *Inorg. Chem.* **1989**, *28*, 373.
(16) Kotowski, M.; Begum, S.; Leipoldt, J. G.; van Eldik, R. *Inorg. Chem.* **1988**, *27*, 4472.
(17) Kotowski, M.; van Eldik, R. *Inorg. Chem.* **1986**, *25*, 3896.
(18) Tubino, M.; Merbach, A. E. *Inorg. Chim. Acta* **1983**, *71*, 149.
(19) Helm, L.; Elding, L. I.; Merbach, A. E. *Helv. Chim. Acta* **1984**, *67*, 1453.
(20) Helm, L.; Elding, L. I.; Merbach, A. E. *Inorg. Chem.* **1985**, *24*, 1719.
(21) Ducommun, Y.; Helm, L.; Merbach, A. E.; Hellquist, B.; Elding, L. I. *Inorg. Chem.* **1989**, *28*, 377.
(22) Baddley, W. H.; Basolo, F. *J. Am. Chem. Soc.* **1966**, *88*, 2944.
(23) Hoechst Analytical Laboratory, Frankfurt, FRG.
(24) Berger, J. Diplomarbeit, University of Frankfurt, 1986.
(25) Fleischmann, F. K.; Conze, E. G.; Stranks, D. R.; Kelm, H. *Rev. Sci. Instrum.* **1974**, *45*, 1427.
(26) van Eldik, R.; Palmer, D. A.; Schmidt, R.; Kelm, H. *Inorg. Chim. Acta* **1981**, *50*, 131.
(27) Amman, C.; Meier, P.; Merbach, A. E. *J. Magn. Reson.* **1982**, *46*, 319.
(28) Frey, U.; Helm, L.; Merbach, A. E. To be submitted for publication.
(29) Bernhard, P.; Helm, L.; Ludi, A.; Merbach, A. E. *J. Am. Chem. Soc.* **1985**, *107*, 312.

Table I. Compositions of Solutions[a]

	soln. no.								
	1	2	3	4	5	6	7	8	9
$[[Pd(Me_5dien)H_2O](ClO_4)_2]$/mol kg^{-1}	0.08	0.08	0.08						
$[[Pd(Et_5dien)H_2O](ClO_4)_2]$/mol kg^{-1}				0.04	0.03	0.08	0.08	0.03	0.08
pH	2.45	3.52	4.30	0.84	1.35	2.46	2.50	2.57	3.84

[a] $[Mn(ClO_4)_2]$/mol kg^{-1} = 0.1; 8 atom % $H_2{}^{17}O$. All concentrations are expressed in molality (moles of solute per kilogram of solvent).

Table II. Derived NMR and Kinetic Parameters for the Variable-Temperature and -Pressure Studies (See Also Table V) of Water Exchange[a]

	$[Pd(Me_5dien)H_2O]^{2+}$	$[Pd(Et_5dien)H_2O]^{2+}$
k_{ex}^{298}/s^{-1}	187 ± 27	2.9 ± 0.1
$\Delta H^{\ddagger}$/kJ mol^{-1}	62.4 ± 3	63.1 ± 1
$\Delta S^{\ddagger}$/J mol^{-1} K^{-1}	7.8 ± 7	−24.6 ± 2
$\Delta V^{\ddagger}$/cm^3 mol^{-1}	−7.2 ± 0.6	−7.7 ± 1.3
$(1/T_{2Q}{}^b)^{298}$/s^{-1}	1390 ± 50	2340 ± 50
E_Q/kJ mol^{-1}	16.6 ± 1.5	18.1 ± 0.6
$\Delta V_Q{}^{\ddagger}$/cm^3 mol^{-1}	−0.8 ± 0.4	−1.0 ± 0.4

[a] Errors represent 1 standard deviation.

so rapidly that its resonance becomes extremely large and is of negligible amplitude, allowing a much better detection of the signal of the water coordinated to the diamagnetic palladium(II) center. It has previously been shown that the addition of Mn^{2+} has no effect on the bound water oxygen relaxation rate.[19] In the slow-exchange limit, the transverse relaxation rate of water bound to a diamagnetic metal center is given by eq 2, where $T_{2Q}{}^b$ is the

$$1/T_2{}^b = 1/T_{2Q}{}^b + 1/\tau \qquad (2)$$

quadrupolar relaxation time and τ is the mean lifetime of water in the first coordination sphere. From transition-state theory the temperature dependence of τ and its relation to the pseudo-first-order exchange rate, k_{ex}, can be expressed by eq 3, where

$$1/\tau = k_{ex} = k_b T/h \exp(\Delta S^{\ddagger}/R - \Delta H^{\ddagger}/RT) \qquad (3)$$

$\Delta S^{\ddagger}$ and $\Delta H^{\ddagger}$ are the entropy and enthalpy of activation, respectively. An Arrhenius temperature dependence can be assumed for the quadrupolar relaxation rate (eq 4, where $(1/T_{2Q}{}^b)^{298}$ is

$$1/T_{2Q}{}^b = (1/T_{2Q}{}^b)^{298} \exp[E_Q{}^b/R(1/T - 1/298.15)] \qquad (4)$$

the contribution at 298.15 K and $E_Q{}^b$ is the corresponding activation energy. All data obtained for $[Pd(Me_5dien)H_2O]^{2+}$ (supplementary material, Table SII) were fitted to eq 2–4 by using a nonlinear least-squares iteration program. The exchange and NMR parameters are listed in Table II. Calculation with the data set from each sample separately showed no significant difference from the parameters given in Table II. The experimental data and calculated curve are illustrated in Figure 2.

For the $[Pd(Et_5dien)H_2O]^{2+}$ complex, $1/T_2{}^b$ is dominated by the quadrupolar relaxation term over most of the temperature domain under study. At high temperature, that is, the interesting kinetic region, the relaxation rate depends irreversibly on the pH for values above 2 (supplementary material, Table SIII and Figure S1). Accordingly the study was performed at pH values of 0.84 and 1.35, for which no dissociation of the complex could be detected in the ^{13}C NMR spectra. To obtain a higher accuracy for the activation parameters, we performed three isotopic labeling experiments at low temperature. The water exchange was followed by monitoring the enrichment of the aqua complex in oxygen-17 after fast injection of oxygen-17-enriched water into a solution of the complex in the presence of Mn^{2+} as relaxation agent. The data were fitted according to eq 5, where $h_{b\infty}$ is the height of the

$$h_b = h_{b\infty}(1 - \exp(-k_{ex}t/(1 - P_m)) \qquad (5)$$

bound water peak at t_∞ and P_m is the mole fraction of coordinated H_2O. The experiments were performed at 274.6 K (solution 5, k_{ex} = 0.29 ± 0.04 s^{-1}) and 275.0 K (solutions 6 and 9, k_{ex} = 0.36 ± 0.05 and 0.28 ± 0.03 s^{-1}, respectively); sample compositions are given in Table I. These low-temperature k_{ex} values were added

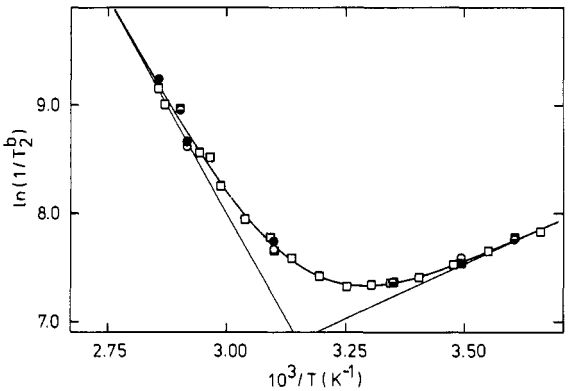

Figure 2. Temperature dependence of $1/T_2{}^b$ (heavy line) from the bound water ^{17}O NMR signals of $[Pd(Me_5dien)H_2O]^{2+}$ solutions at different pH values with $1/\tau$ (light line, left) and $1/T_{2Q}{}^b$ (light line, right) components. The numbers refer to the sample compositions given in Table I: (○) solution 1; (□) solution 2; (●) solution 3.

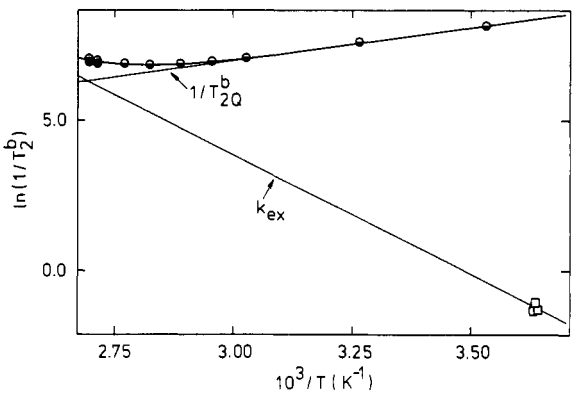

Figure 3. Temperature dependence of $1/T_2{}^b$ from the bound water ^{17}O NMR signal of $[Pd(Et_5dien)H_2O]^{2+}$ solutions at different pH. The numbers refer to the sample compositions given in Table I: (○) $T_2{}^b$, solution 4; (●) $T_2{}^b$, solution 8; (□) k_{ex} obtained from fast-injection experiments.

to the $1/T_2{}^b$ data, and a combined analysis of all results gave the final set of quadrupolar relaxation and exchange parameters listed in Table II and Figure 3.

Variable Pressure. The pressure dependence of ln k_{ex} can be described by the linear equation (6), since we can assume that the corresponding volumes of activation are pressure independent, as is usual for simple solvent-exchange reactions.[30] $(k_{ex})_0$ is the

$$\ln k_{ex} = \ln (k_{ex})_0 - P\Delta V^{\ddagger}/RT \qquad (6)$$

exchange rate constant at zero pressure. A similar equation, eq 7, describes the pressure dependence of the quadrupolar relaxation

$$\ln (1/T_{2Q}{}^b) = \ln (1/T_{2Q}{}^b)_0 - \Delta V_Q{}^{\ddagger}P/RT \qquad (7)$$

rate as a function of the quadrupolar activation volume $\Delta V_Q{}^{\ddagger}$ and the contribution at zero pressure $(1/T_{2Q}{}^b)_0$. The transverse relaxation rate was determined at pressures up to 200 MPa. We measured each complex at two temperature domains to define the quadrupolar (low-temperature) and kinetic (high-temperature)

(30) Ducommun, Y.; Newmann, K. E.; Merbach, A. E. *Inorg. Chem.* **1980**, *19*, 3696.

Table III. Relaxation Rates, $1/T_2^b$, of the Bound Water ^{17}O NMR Signal of $[Pd(Me_5dien)H_2O]^{2+}$ at Variable Pressure and at Different Temperatures (Solution 2: Composition Given in Table I)

P/MPa	$(1/T_2^b)/s^{-1}$ [a]	P/MPa	$(1/T_2^b)/s^{-1}$ [b]	P/MPa	$(1/T_2^b)/s^{-1}$ [c]	P/MPa	$(1/T_2^b)/s^{-1}$ [d]
0.1	1826	0.1	1756	0.1	2161	0.1	2325
0.1	1828	36	1831	0.1	2062	0.1	2552
40	1819	71	1843	45	2331	35	2772
82	1908	105	1873	82	2298	72	2703
119	1862	140	1899	119	2800	107	2933
161	1911	158	1912	162	3039	142	3104
200	2000	200	1997	201	2949	167	3450
						189	3614

[a] T = 286.7 K. [b] T = 288.2 K. [c] T = 320.4 K. [d] T = 323.4 K.

Table IV. Relaxation Rates, $1/T_2^b$, of the Bound Water ^{17}O NMR Signal of $[Pd(Et_5dien)H_2O]^{2+}$ at Variable Pressure and at Different Temperatures (Composition of Solutions Given in Table I)

P/MPa	$(1/T_2^b)/s^{-1}$ [a]	P/MPa	$(1/T_2^b)/s^{-1}$ [b]	P/MPa	$(1/T_2^b)/s^{-1}$ [c]
0.1	1265	0.1	1261	0.1	1035
0.1	1218	0.1	1276	0.1	994
12	1352	40	1233	35	1120
37	1277	80	1290	72	1146
69	1351	119	1289	103	1133
112	1400	162	1413	140	1208
139	1361	196	1357	163	1221
169	1399			197	1429
196	1338				

[a] T = 326.0 K, solution 7. [b] T = 326.8 K, solution 6. [c] T = 369.4 K, solution 7.

pressure dependences. All experimental data are reported in Tables III and IV. The low temperature was chosen in a region where the kinetic contribution to $1/T_2^b$ is very small (<4%). At the high temperature both the kinetic and quadrupolar contributions comprise about 50% of $1/T_2^b$. We fitted all the data for each complex simultaneously to eq 2, 6, and 7. In theory, $(k_{ex})_0$ and $(1/T_{2Q}^b)_0$ at each temperature could be fixed at the values obtained from the variable-temperature analysis. In practice, small differences in temperature calibration between the variable-temperature and variable-pressure experiments could cause nonrandom errors in the $1/T_2^b$ measurements. Thus, those parameters that contributed the smaller part of ΔV^* values were fixed at their atmospheric-pressure values. The $(1/T_{2Q}^b)_0$ and $(k_{ex})_0$ values (fixed and fitted) are reported in Table V, and the corresponding activation volumes are given in Table II.

Anation Reactions. The neutral ligands selected for the anation reactions according to eq 8 and L = $SC(NH_2)_2$, $SC(NHMe)_2$, and $SC(NMe_2)_2$. The reactions are accompanied by characteristic

$$[Pd(R_5dien)H_2O]^{2+} + L \xrightarrow{k_{an}} [Pd(R_5dien)L]^{2+} + H_2O \quad (8)$$

UV–vis spectral changes and clean isosbestic points, for instance at 327 and 372 nm for R = Et and L = $SC(NH_2)_2$. In this case the reaction is slow enough to be recorded as a function of time on a conventional spectrophotometer. In some cases, subsequent slow substitution reactions were observed,[24] especially at pH ≤ 4 and in the presence of a large excess of L, which were assigned to the ring opening of the dien ligand due to the labilizing properties of S-coordinated ligands.[9] The anation reactions could be studied without any complications in the range 4.5 ≤ pH ≤ 5.5 and [L] ≤ 0.02 M for [Pd(II)] ≥ 1 × 10^{-4} M (always at least 10-fold excess of L). The pseudo-first-order rate plots were linear for at least 2–3 half-lives of the reaction. The observed rate constants are summarized as a function of [L] in Table SIV. Plots of k_{obsd} versus [L] are linear and exhibit no meaningful intercepts such that the anation rate constant k_{an} could be calculated from the slope of such plots according to eq 9. The temperature and

$$k_{obsd} = k_{an}[L] \quad (9)$$

pressure dependencies of k_{an} along with the calculated activation parameters are summarized in Table VI. The plots of ln k_{an} versus pressure were linear within the experimental error limits in all cases.

Efforts were undertaken to study the reverse aquation reaction of (8) in order to measure ΔV^* for this process, which would enable the construction of an overall volume profile for the forward and reverse steps.[2,31] However, the subsequent substitution reactions that occur on a longer time scale, even at low [L], complicate these measurements in most cases. Only in the case of the $[Pd(Me_5dien)SC(NMe_2)_2]^{2+}$ complex could we measure the aquation reaction by treating it with 0.01 M NaOH. Under such conditions the observed rate constant represents the aquation rate constant[5] since almost no $[OH^-]$ dependence was observed. The pressure dependence of the observed rate constant is reported in Table VIII along with the estimated volume of activation.

Discussion

The pK_a values of 7.19 ± 0.03 and 7.53 ± 0.09 for the $[Pd(Me_5dien)H_2O]^{2+}$ and $[Pd(Et_5dien)H_2O]^{2+}$ species, respectively, determined from the pH dependence of the $^{13}C\{^1H\}$ chemical shifts (Figure 1) are in good agreement with the values of 7.29 ± 0.02 and 7.47 ± 0.05, respectively, determined spectrophotometrically at 25 °C and 0.1 M ionic strength.[7,14] It follows from these values that the aqua complexes are the main reactive species at pH ≤ 5, where all the kinetic work was performed. The anation rate constants for these complexes decrease drastically at pHs above the pK_a value due to the formation of stable hydroxo complexes.[13,14]

A comparison of the water-exchange data available for aqua complexes of Pd(II), given in Table VII, reveals that the introduction of the dien ligand on the Pd(II) center increases the rate of solvent exchange by 1 order of magnitude. Introducing methyl and ethyl groups on the dien ligand causes a meaningful decrease in k_{ex}, which is accompanied by an increase in ΔH^* and a more

Table V. Derived NMR and Kinetic Parameters for the Variable-Pressure Studies of Water Exchange (See Also Table II)

	T/K	$(1/T_{2Q}^b)_0/s^{-1}$	% $(1/T_{2Q}^b)_0$ [a]	$(k_{ex})_0/s^{-1}$	% $(k_{ex})_0$ [a]
$[Pd(Me_5dien)H_2O]^{2+}$	286.7	1741 ± 34	96	(65)	4
	288.2	1719 ± 36	96	(68)	4
	320.4	(868)	41	1259 ± 36	59
	323.4	(825)	34	1612 ± 43	66
$[Pd(Et_5dien)H_2O]^{2+}$	326.0	1252 ± 21	98	(28)	2
	326.8	1222 ± 23	98	(30)	2
	369.4	(573)	56	449 ± 21	44

[a] Each contribution is expressed as a percentage of the value of $1/T_2^b$. The values within parentheses were fixed during the fitting procedure.

Table VI. Rate and Activation Parameters as a Function of Temperature and Pressure for the reaction[a]

$$[Pd(R_5dien)H_2O]^{2+} + L \xrightarrow{k_{an}} [Pd(R_5dien)L]^{2+} + H_2O$$

R	L	T/K	P/MPa	k_{an}/M^{-1} s^{-1}	$\Delta H^{\ddagger}$/kJ mol^{-1}	$\Delta S^{\ddagger}$/J K^{-1} mol^{-1}	$\Delta V^{\ddagger}$/cm^3 mol^{-1}
Me	$SC(NH_2)_2$	289.4	0.1	1073 ± 34	30.1 ± 1.2	−85 ± 4	
		293.1		1211 ± 33			
		298.1		1583 ± 46			
		303.1		1905 ± 60			
		308.1		2395 ± 68			
		288.1	5	1138 ± 40			−9.4 ± 0.4
			25	1234 ± 17			
			50	1357 ± 26			
			75	1471 ± 27			
			95	1636 ± 70			
	$SC(NHMe)_2$	289.4	0.1	452 ± 40	34.2 ± 0.8	−79 ± 2	
		293.1		550 ± 16			
		298.1		718 ± 28			
		303.1		884 ± 16			
		308.1		1136 ± 38			
		298.1	5	770 ± 22			−9.1 ± 0.6
			25	862 ± 11			
			50	914 ± 16			
			75	1005 ± 17			
			95	1090 ± 27			
	$SC(NMe_2)_2$	289.2	0.1	119 ± 2	36.8 ± 0.8	−81 ± 2	
		293.1		145 ± 4			
		298.1		195 ± 5			
		303.1		251 ± 8			
		308.1		315 ± 5			
		298.1	5	196 ± 8			−13.4 ± 0.7
			20	201 ± 7			
			40	235 ± 8			
			60	259 ± 2			
			80	284 ± 5			
			97	319 ± 8			
Et	$SC(NH_2)_2$	288.1	0.1	0.53 ± 0.01	53.5 ± 2.0	−69 ± 7	
		293.1		0.74 ± 0.04			
		298.1		1.12 ± 0.04			
		302.6		1.59 ± 0.03			
		288.1	3	0.64 ± 0.01			−8.4 ± 0.3
			20	0.67 ± 0.01			
			40	0.74 ± 0.01			
			60	0.79 ± 0.03			
			80	0.84 ± 0.04			
			100	0.90 ± 0.04			
	$SC(NHMe)_2$	288.1	0.1	0.239 ± 0.001	58.5 ± 0.8	−58 ± 2	
		293.1		0.35 ± 0.02			
		298.1		0.54 ± 0.01			
		302.7		0.75 ± 0.01			
		307.7		1.13 ± 0.01			
		288.1	3.5	0.311 ± 0.003			−10.2 ± 0.6
			10	0.339 ± 0.003			
			20	0.347 ± 0.009			
			40	0.380 ± 0.006			
			60	0.407 ± 0.003			
			80	0.449 ± 0.003			
			100	0.479 ± 0.017			
	$SC(NMe_2)_2$	288.1	0.1	0.049 ± 0.001	63.1 ± 1.2	−56 ± 4	
		293.1		0.076 ± 0.001			
		298.1		0.117 ± 0.002			
		303.1		0.190 ± 0.002			
		308.1		0.275 ± 0.007			
		298.1	5	0.116 ± 0.002			−12.7 ± 0.6
			20	0.125 ± 0.003			
			40	0.142 ± 0.003			
			60	0.152 ± 0.001			
			80	0.176 ± 0.001			
			100	0.186 ± 0.005			

[a] Experimental conditions as indicated in Table SIV (supplementary material); ionic strength 0.1 M.

negative $\Delta V^{\ddagger}$. A similar trend was also found for the investigated anation reactions (see further discussion), from which it follows that an increase in steric hindrance on the dien ligand hinders the associative attack of the entering nucleophile, i.e. the solvent in the present case. A similar 6 orders of magnitude decrease in the solvolysis rate constant of complexes of the type $[Pd(R_5dien)Cl]^+$ (R = H, Me, Et), as one goes from dien to Et_5dien, was reported before.[5] Noteworthy is the fact that here too the decrease in rate

(31) Hellquist, B.; Elding, L. I.; Ducommun, Y. *Inorg. Chem.* **1988**, *27*, 3620.

Table VII. Rate and Activation Parameters for Water Exchange on Aqua Complexes of Pd(II)

complex	k_{ex}(298.1 K)/s^{-1}	$\Delta H^{\ddagger}$/kJ mol^{-1}	$\Delta S^{\ddagger}$/J K^{-1} mol^{-1}	$\Delta V^{\ddagger}$/cm^3 mol^{-1}	ref
$Pd(H_2O)_4^{2+}$	560 ± 40	49 ± 2	−26 ± 6	−2.2 ± 0.2	19
$Pd(dien)H_2O^{2+}$	5100 ± 60	38 ± 1	−47 ± 3	−2.8 ± 0.5	34
$Pd(Me_5dien)H_2O^{2+}$	187 ± 27	62 ± 3	+8 ± 7	−7.2 ± 0.6	this work
$Pd(Et_5dien)H_2O^{2+}$	2.9 ± 0.1	63 ± 1	−25 ± 2	−7.7 ± 1.3	this work

Table VIII. Pressure Dependence of the Aquation Rate Constant[a] for $[Pd(Me_5dien)SC(NMe_2)_2]^{2+}$

P/MPa	$10^4 k_{aq}$/s^{-1} [b]	$\Delta V^{\ddagger}$/cm^3 mol^{-1}
5	6.01 ± 0.09	−4.5 ± 0.4
20	6.04 ± 0.06	
40	6.28 ± 0.09	
60	6.61 ± 0.13	
80	6.74 ± 0.11	
100	7.12 ± 0.12	

[a] T = 298.1 K; ionic strength 0.1 M; $[OH^-]$ = 0.01 M. [b] Mean value of at least two kinetic runs.

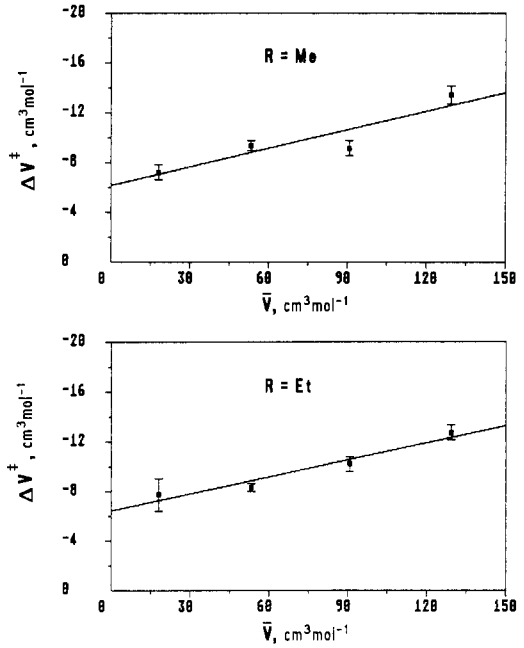

Figure 4. Plot of $\Delta V^{\ddagger}$ for water exchange on and the anation of $[Pd(R_5dien)H_2O]^{2+}$ versus the partial molar volume of the entering ligand. Data were taken from Tables II and VI and ref 24.

constant was accompanied by a significant increase in $\Delta H^{\ddagger}$ and almost constant, significantly negative, $\Delta S^{\ddagger}$ and $\Delta V^{\ddagger}$ values, demonstrating the operation of an associative reaction mode throughout the series of complexes. When the steric hindrance on such complexes is increased, the nucleophile-dependent reaction path (usually referred to as the k_2 path) disappears and the substitution reaction mainly proceeds via the nucleophile-independent reaction path (k_1 path), i.e. solvolysis.[5,22,32] The more negative $\Delta V^{\ddagger}$ values reported for water exchange on the substituted dien complexes in Table VII demonstrate the more effective overlap of the van der Waals radii of the reactant molecules during the associative water-exchange process on these complexes. This means that the significantly larger coordination sphere of the Me_5dien and Et_5dien complexes can accommodate the entering solvent molecule more effectively on a volume basis than the smaller unsubstituted complex.

The anation reactions studied in this investigation all involve the substitution of neutral ligands. In this way the interpretation of the activation parameters, especially $\Delta V^{\ddagger}$, is significantly simplified since major changes in electrostriction during such

(32) Goddard, J. B.; Basolo, F. *Inorg. Chem.* **1968**, *7*, 936.

Table IX. Summary of Available $\Delta V^{\ddagger}$ Data for the Reaction

$$[Pd(R_5dien)H_2O]^{2+} + L^{n-} \underset{k_{aq}}{\overset{k_{an}}{\rightleftharpoons}} [Pd(R_5dien)L]^{(2-n)+} + H_2O$$

R	L^{n-}	$\Delta V^{\ddagger}(k_{an})$	$\Delta V^{\ddagger}(k_{aq})$	$\Delta \bar{V}$[a]	ref
Me	H_2O	−7.2 ± 0.6	−7.2 ± 0.6	0	*b*
	$SC(NH_2)_2$	−9.3 ± 0.4			*b*
	$SC(NHMe)_2$	−9.1 ± 0.6			*b*
	$SC(NMe_2)_2$	−13.4 ± 0.7	−4.5 ± 0.4	−8.9 ± 1.1	*b*
	Cl^-	−4.9 ± 0.4	−11.6 ± 0.5	+6.7 ± 0.9	15
	Br^-	−7.3 ± 0.4	−11.4 ± 0.7	+4.1 ± 1.1	15
	I^-	−9.9 ± 1.2	−9.7 ± 0.3	−0.2 ± 1.5	15
	N_3^-	−10.1 ± 0.3	−11.4 ± 0.7	+1.3 ± 1.0	15
	$C_2O_4^{2-}$	−5.9 ± 0.4	−10.4 ± 0.6	+4.5 ± 1.0	15
Et	H_2O	−7.7 ± 1.3	−7.7 ± 1.3	0	*b*
	$SC(NH_2)_2$	−8.3 ± 0.3			*b*
	$SC(NHMe)_2$	−10.2 ± 0.6			*b*
	$SC(NMe_2)_2$	−12.7 ± 0.6			*b*
	Cl^-	−5.9 ± 0.3	−11.6 ± 0.2	+5.7 ± 0.5	15
				+4.9 ± 0.8[c]	15
	Br^-	−5.8 ± 0.4	−11.6 ± 0.5	+5.8 ± 0.9	15
	I^-	−7.0 ± 0.6	−6.8 ± 0.9	−0.2 ± 1.5	15
	N_3^-	−11.0 ± 0.4	−11.3 ± 0.4	−0.3 ± 0.8	15
	$C_2O_4^{2-}$	−3.9 ± 0.2	−7.6 ± 0.8	+3.7 ± 1.0	15

[a] $\Delta \bar{V} = \Delta V^{\ddagger}(k_{an}) - \Delta V^{\ddagger}(k_{aq})$ unless otherwise indicated. [b] This work. [c] Determined from the pressure dependence of the equilibrium constant.

reactions in water as solvent are not expected.[2,16,17,31] The results in Table VI clearly demonstrate how k_{an} decreases with increasing steric hindrance on the dien ligand and on the entering thiourea ligand. This decrease in k_{an} is accompanied by a significant increase in $\Delta H^{\ddagger}$, reflecting the difficulties encountered by the entering ligand in binding to the metal center during an associative substitution process as found before.[5] The values of $\Delta V^{\ddagger}$ become more negative for the larger entering ligands. This is demonstrated for the solvent-exchange and anation reactions of $[Pd(Et_5dien)H_2O]^{2+}$ in Figure 4 by plotting $\Delta V^{\ddagger}$ versus $\bar{V}$, the partial molar volume of the entering ligand as determined from density measurements.[24] A similar correlation exists for the corresponding data for the Me_5dien complex. It follows that with increasing partial molar volume of the entering ligand the overlap of the van der Waals radii increases during bond formation and results in a more negative $\Delta V^{\ddagger}$.

All the available activation volume data for the anation and reverse aquation reactions of $[Pd(Me_5dien)H_2O]^{2+}$ and $[Pd(Et_5dien)H_2O]^{2+}$ are summarized in Table IX. For the anation reactions involving anionic entering ligands, the intrinsic volume decrease during associative bond formation is partially offset by a volume increase due to a decrease in electrostriction resulting from charge neutralization. This effect is even more significant in the case of the anation by oxalate. The data for the anation by the 1− charged ions also exhibit the increase in the absolute value of $\Delta V^{\ddagger}$ with increasing partial molar volume of the entering ligand as found for the neutral ligands studied in this investigation. The values of $\Delta V^{\ddagger}$ for the reverse aquation reactions are also affected by the nature of the leaving group, an aspect that has been treated in detail elsewhere.[17] The value of −4.5 ± 0.4 cm^3 mol^{-1} reported here for the aquation of $[Pd(Me_5dien)SC(NMe_2)_2]^{2+}$ is very close to that reported for closely related complexes with NH_3 and pyridine as leaving groups.[17] Significantly more negative values are in general observed for complexes with anionic leaving groups.[17] The values of $\Delta V^{\ddagger}(k_{an})$ and $\Delta V^{\ddagger}(k_{aq})$ can be combined to estimate the overall reaction volume $\Delta \bar{V}$, which has values between 0 and +6 cm^3 mol^{-1} for complexes with anionic leaving groups.[15] A significantly more negative value

of ca. -9 cm^3 mol^{-1} is now reported for this reaction involving a neutral leaving group. It follows that this value indicates the volume decrease on substituting a water molecule ($\bar{V} = 18$ cm^3 mol^{-1}) with $SC(MNe_2)_2$ ($\bar{V} = 130$ cm^3 mol^{-1}) on a square-planar metal ion. The significantly more positive values observed for the other systems quoted in Table IX can be ascribed to an increase in molar volume due to charge neutralization and a decrease in electrostriction for these reactions.

The results of this investigation are in good agreement with those reported recently[31] for solvent exchange on and anation of $Pd(H_2O)_4^{2+}$ by MeCN and Me_2SO. Here too, ΔV^* decreases along the series, viz. -2.2 ± 0.2 (H_2O), -4.0 ± 0.8 (MeCN), and -9.2 ± 0.6 cm^3 mol^{-1} (Me_2SO), compared to almost constant values for the reverse aquation reactions, viz. -2.2 ± 0.2 (H_2O), -1.5 ± 0.5 (MeCN), and -1.7 ± 0.6 cm^3 mol^{-1} (Me_2SO). The construction of a volume profile for the anation of $[Pd(Me_5dien)H_2O]^{2+}$ by $SC(NMe_2)_2$ reveals that the transition state for the forward and reverse reaction is significantly more compact than either the reactant or product states. A similar finding was reported for the other anation reactions included in Table IX[15] as well as for those of $Pd(H_2O)_4^{2+}$ mentioned above.[31] It follows that the solvent exchange and anation data reported in this study once again underline the operation of an associative substitution mechanism in these systems. The results of this investigation also demonstrate that steric hindrance on the dien ligand can slow down the ligand substitution process significantly but does not change the basic nature of the mechanism. Earlier work[5,7,15] has demonstrated this more explicitly for an extended series of complexes. It has been suggested[33] that strong nucleophiles can in some cases overcome the steric barrier. However, bulky entering groups, even when they are strong nucleophiles, can be less effective than small ligands having poor nucleophilicity but being capable of penetrating the coordination sphere.

Acknowledgment. R.v.E. gratefully acknowledges financial support from the Deutsche Forschungsgemeinschaft, the Fonds der Chemischen Industrie, and the Volkswagen-Stiftung. A.E.M. thanks the Swiss National Science Foundation for financial support.

Registry No. $[Pd(Me_5dien)H_2O]^{2+}$, 85344-11-2; $[Pd(Et_5dien)H_2O]^{2+}$, 118169-65-6; $SC(NH_2)_2$, 62-56-6; $SC(NHMe)_2$, 534-13-4; $SC(NMe_2)_2$, 2782-91-4; H_2O, 7732-18-5.

Supplementary Material Available: Tables of the chemical shift as a function of pH, the relaxation rate as a function of temperature at various pH values, and rate constants for the anation reactions as a function of ligand concentration and a figure presenting the temperature dependence of the relaxation rate at various pH values (6 pages). Ordering information is given on any current masthead page.

(33) Canovase, L.; Cusumano, M.; Giannetto, A. *J. Chem. Soc., Dalton Trans.* **1983**, 195.
(34) Helm, L.; Merbach, A. E.; Kotowski, M.; van Eldik, R. *High Pressure Res.*, in press.

Notes

Contribution from the School of Chemical Sciences, University of East Anglia, Norwich NR4 7TJ, U.K.

Structure and Vibrational Spectra of $NF_4^+BF_4^-$: A Reappraisal

Mona Arif† and Sidney F. A. Kettle*

Received March 21, 1989

In a recent publication in this journal,[1] a fascinating problem was posed on connection with the reconciliation between the crystal structure and vibrational spectra of $NF_4^+BF_4^-$. This compound crystallizes in the $P\bar{4}2_1m$ space group with $Z = 4$. In contrast, the infrared and Raman spectra of the crystal are consistent with a uniaxial space group with $Z = 1$, although the authors did not summarize the spectral observations in this way. In order to reconcile these rather different results, the authors postulated the occurrence of a rotation or large amplitude oscillation of the BF_4^- groups about one B–F bond so that they have an effective C_{3v} symmetry, in contrast to their crystallographic C_s site symmetry, and that the vibrations take place within this rotationally smeared-out environment. They used this model to explain not only the simple BF_4^- anion spectrum but also the NF_4^+ spectrum, the latter ion occupying two distinct sites, one of C_{2v} symmetry and the other of S_4 symmetry (although the molecule in the latter site is actually of strict D_{2d} symmetry). However, there is one significant problem with this model that was not discussed: the problem of time scale. Typically, a rotation is rather slower than a vibrational motion—the corresponding transitions occur in different spectral regions. One additional consequence of the model is therefore that some, if not all, of the vibrations explore a wide range of rotationally different local environments and so should show a marked broadening. In fact, the spectra reported have quite normal band widths. We believe that there is an alternative explanation of the spectroscopic observations. Our explanation is based, in part, on the recognition that a vibrational space group may differ from the crystallographic one.[2] In the present case it is important also to recognize certain crystal structure insensitive aspects of vibrational spectroscopy. Finally, we take this opportunity to present a method of analysis appropriate when more than one site is occupied by chemically equivalent groups (in the present case, NF_4^+).

Although our conclusions do not strictly depend upon it, it is simplest to assume that there is strong vibrational coupling between NF_4^+ groups and, separately, between BF_4^-. In making this assumption we follow Christe et al.;[1] without it the problem that arises is much less severe—all spectra are expected to be site-symmetry determined and so the only residual problem arises from the C_{2v}–S_4 duality of the NF_4^+ sites. Let us first consider the NF_4^+ ions. All are arranged with a tetrahedral 2-fold axis along the crystallographic z axis. Further, sets of four NF_4^+ cations, two on C_{2v} sites and two on S_4 sites, are coplanar to ± 0.05 Å along z, and, within error, are interrelated by an S_4 operation of the space group $P\bar{4}2m$ (D_{2d}^1) with $Z = 1$. Of course, NF_4^+ groups on C_{2v} and S_4 sites differ in their static geometries, but these differences can be ignored. There are two reasons for this. First, the zero-point and lattice vibrational motions both will tend to smear out the static distinctions. Second, vibrational coupling, which, it is generally accepted, is expected to occur, will mean that normal coordinates involve both types of NF_4^+ groups; their individuality is lost. The spectra reported are entirely consistent with the conclusion that the NF_4^+ groups subtend a $P\bar{4}2m$ (D_{2d}^1) vibrational space group with $Z = 1$. The observed splitting of NF_4^+ T_2 modes into two components with a 2:1 intensity ratio, is entirely consistent with $D_d \rightarrow D_{2d}$ ($T_2 \rightarrow E + B_2$), as is the splitting of the E (T_d) mode into two peaks of equal intensity ($E \rightarrow A_1 + B_1$). Finally, the analysis requires coincident infrared and Raman peaks when both are active, as observed.

The analysis of the NF_4^+ features that we have just presented is the simplest available. At a more detailed level, we may wish

† On leave from Universidade da Beira Interior, Covilha, Portugal.

(1) Christe, K. O.; Lind, M. D.; Thorup, N.; Russell, D. R.; Fawcett, J.; Bau, R. *Inorg. Chem.* **1988**, *27*, 2450.
(2) Ismail, M. A.; Jayasooriya, U. A.; Kettle, S. F. A. *J. Chem. Phys.* **1983**, *79*, 4459.

0020-1669/89/1328-3765$01.50/0